Acceptor Helix Interactions in a Class II tRNA Synthetase: Photoaffinity Cross-Linking of an RNA Miniduplex Substrate†

Karin Musier-Forsyth‡ and Paul Schimmel*

Department of Biology, Massachusetts Institute of Technology, Cambridge, Massachusetts 02139

Received September 3, 1993; Revised Manuscript Received November 4, 1993®

ABSTRACT: The 875 amino acid class II *Escherichia coli* alanine tRNA synthetase aminoacylates hairpin minihelices and miniduplexes comprising complementary base pairs that reconstruct the acceptor helix of alanine tRNA. Aminoacylation is dependent upon a G3:U70 base pair in the tRNA acceptor stem. A synthetic RNA miniduplex with a phosphorothioate internucleotide linkage on the 5′-side of U70 facilitated the stable attachment of a pendant benzophenone to the ribonucleotide backbone. The benzophenone-labeled duplex is active for aminoacylation. Irradiation of the labeled duplex produced a cross-linked RNA protein complex, in which the major site of RNA attachment is the segment between the class II defining sequence motifs 2 and 3. This segment spans a putative zinc-binding motif, which has been implicated in acceptor helix recognition, and is within a 461 amino acid N-terminal fragment that was recently shown to have full activity for minihelix aminoacylation. These results, together with the X-ray crystallographic investigations of the class II aspartate tRNA synthetase–tRNA^{Asp} complex, suggest that the segment between motifs 2 and 3 in the 10 class II synthetases contributes generally to the docking of tRNA acceptor helices. The sequence diversity of this segment implies that its mode of interaction with the acceptor helix is idiosyncratic to the class II enzyme.

We report here the results of a biochemical approach to identify the region in a class II tRNA synthetase that interacts with the acceptor helix of its cognate tRNA. Transfer RNA molecules fold into two domains arranged at right angles to form an L-shaped structure (Rich & RajBhandary, 1976). These domains are the acceptor-TψC minihelix and the anticodon–dihydrouridine stem–biloop. Aminoacyl tRNA synthetases can also be viewed to a first approximation as comprising two major domains, one of which contains the catalytic site and the region needed for acceptor helix interactions (Schimmel et al., 1993). On the basis of the structure of this domain, the enzymes are divided into two classes of 10 enzymes each (Schimmel, 1987; Cusack et al., 1990; Eriani et al., 1990). These classes are defined by limited sequence motifs, which are shared by members of the same class and which encode structural motifs that form part of the catalytic site. This domain has a similar structure for each member of the same class, even though the class-defining sequence elements generally constitute only 10% or less of the total primary structure of the catalytic domain. Joined to the catalytic domain is a large nonconserved structure that differs even for members of the same class. In at least some synthetases, this nonconserved structure provides contacts with the more distal (to the 3′-amino acid attachment site) part of the tRNA, including the anticodon (Brunie et al., 1990; Rould et al., 1991; Ruff et al., 1991).

The two major domains of synthetases thus appear to correspond to the two domains of the L-shaped tRNA molecule. For seven synthetases, the acceptor-TψC minihelix domain is a substrate for specific aminoacylation, with the specificity of aminoacylation corresponding to the acceptor-TψC sequence of the corresponding tRNA. These enzymes include alanine, glycine, histidine, isoleucine, methionine, serine, and valine tRNA synthetases (Francklyn & Schimmel, 1989, 1990; Francklyn et al., 1992; Frugier et al., 1992; Martinis & Schimmel, 1992; Nureki et al., 1993; Sampson & Saks, 1993). In some instances, such as the alanine, glycine, histidine, and methionine tRNA synthetases, RNA hairpin oligonucleotides with as few as 4 or 5 base pairs have been shown to be specifically aminoacylated (Shi et al., 1992). Aminoacylation efficiency and specificity are generally dependent on the "discriminator" base N73 and 1–2 base pairs. The aminoacylation of RNA oligonucleotides has suggested the concept of an operational RNA code for amino acids which, in turn, may be related to the genetic code and its historical development (Schimmel et al., 1993).

Although sequence-specific aminoacylation of RNA oligonucleotides has been demonstrated in seven different systems, little is known about the specific RNA–protein contacts responsible for the discrimination observed at the binding step and in the transition state of catalysis. In the class I *Escherichia coli* glutamine tRNA synthetase in complex with tRNA^{Gln}, an insertion into the catalytic domain provides acceptor helix contacts, while interactions with the anticodon occur through the nonconserved β-barrel domain, which is fused to the C-terminal side of the catalytic domain (Rould et al., 1989, 1991). In the class II yeast aspartate tRNA synthetase–tRNA^{Asp} cocrystal, acceptor helix contacts also occur with residues incorporated into the conserved catalytic domain, and contacts with the anticodon are made through a nonconserved structure that is joined to the N-terminal side of the catalytic domain (Ruff et al., 1991; Cavarelli et al., 1993). In both systems, residues not conserved between members of the same class are involved in RNA interactions.

† This work was supported by Grant Number GM15539 from the National Institutes of Health.

* Author to whom correspondence should be addressed. Telephone: (617) 253-6739. FAX: (617) 253-6636.

‡ K.M.-F. was an American Cancer Society Postdoctoral Fellow. Present address: Department of Chemistry, University of Minnesota, 207 Pleasant Street S.E., Minneapolis, MN 55455-0431.

® Abstract published in *Advance ACS Abstracts*, January 1, 1994.

0006-2960/94/0433-773$04.50/0

The experiments reported here were focused on *E. coli* alanine tRNA synthetase (AlaRS[1]), an α_4 tetramer of identical polypeptides. This enzyme is one of the aforementioned seven which efficiently and specifically aminoacylate acceptor stem helices. The G3:U70 base pair in the acceptor stem of $tRNA^{Ala}$ is the major determinant for aminoacylation with alanine (Hou & Schimmel, 1988; McClain & Foss, 1988; Francklyn & Schimmel, 1989). The G3:U70 base pair is conserved in evolution among alanine tRNAs in prokaryotes and in the cytoplasm of eukaryotes (Hou & Schimmel, 1989; Trezeguet et al., 1991). Transfer of this base pair into other tRNAs confers alanine acceptance on them. Moreover, the enzyme will aminoacylate short RNA duplexes that recapitulate the acceptor end of $tRNA^{Ala}$ (Francklyn & Schimmel, 1989; Musier-Forsyth et al., 1991a,b). The aminoacylation of these model substrates is G3:U70-dependent. Using substrates containing base analogs and deoxynucleotides introduced at specific positions, the primary site of recognition was localized to the unpaired exocyclic 2-amino group of G3. Additional functional contacts occur with the 2-amino group of G2 (in a G2:C71 base pair) and three 2′-hydroxyl groups which are within a 5-Å radius of the critical G3 2-amino group (Musier-Forsyth et al., 1991b; Musier-Forsyth & Schimmel, 1992).

Although the region in AlaRS that makes contact with the acceptor helix recognition elements has not been identified, an N-terminal 461 amino acid monomeric fragment of AlaRS contains the three conserved sequence motifs that are characteristic of class II enzymes and has full activity for the aminoacylation of an RNA minihelix (Buechter & Schimmel, 1993). Thus, the missing 414 C-terminal residues with the oligomerization domain neither directly nor indirectly affect interaction with the acceptor-TψC stem. That the catalytic domain contains all of the contacts for minihelix interactions is consistent with the aforementioned structural studies of the tRNA cocrystals of glutamine tRNA synthetase and aspartate tRNA synthetase.

In these studies, we used a photo-cross-linking probe to localize approximately the region of AlaRS which makes contact with the acceptor helix. A benzophenone photoaffinity label was attached next to the critical G3:U70 base pair, at a position where its attachment does not disrupt aminoacylation of the model RNA substrate. This active substrate was irradiated in the presence of the enzyme, and the peptide cross-linked to the protein was identified. The results obtained support the concept that idiosyncratic insertions into the catalytic domain form structures that interact with the minihelix domain. Together with the aforementioned structural analysis of aspartate tRNA synthetase, these observations also suggest that the recruitment of idiosyncratic acceptor helix-binding insertions next to the site of the activated amino acid may have been a general mechanism for the historical development of an operational RNA code for amino acids.

MATERIALS AND METHODS

Protein Purification and Assays. Wild-type *E. coli* alanine tRNA synthetase was purified as previously described (Miller et al., 1991). Protein concentrations were based on active-site titrations using the adenylate burst assay (Fersht et al., 1975). Aminoacylation and ATP–P_i exchange assays were performed as described (Hill & Schimmel, 1989; Musier-Forsyth et al., 1991a). TPCK-treated trypsin was purchased from Worthington Biochemical Corporation and further purified to remove trace RNase contaminants as described (Hill & Schimmel, 1989).

Ribonucleic Acids. E. coli $tRNA^{Ala}$ was purchased from Subriden RNA. Minihelix RNA substrates were prepared by *in vitro* transcription using T7 RNA polymerase, as described (Milligan et al., 1987; Shi et al., 1990), and purified on 16% polyacrylamide gels. All duplex RNA and mixed DNA–RNA substrates were prepared by chemical synthesis of oligonucleotides on a Gene Assembler Plus (Pharmacia) using the phosphoramidite method (Scaringe et al., 1990). Single phosphorothioate diesters were introduced into oligonucleotides by replacing the sulfurization reagent tetraethylthiuram disulfide (TETD) (Applied Biosystems) for the oxidation reagent in the synthesis cycle and employing a 15-min reaction time. The presence of a single phosphorothioate diester was confirmed by ^{31}P NMR. Integration of the phosphorothioate diastereomer resonances at approximately 56 ppm and the phosphodiester region at about 0 ppm (relative to H_3PO_4) yielded close to the expected 11:1 ratio of phosphodiester:phosphorothioate.

Preparation of Benzophenone-Labeled Oligonucleotide. A primarily ribonucleotide tridecamer corresponding to the 3′-end of $tRNA^{Ala}$ containing a single phosphorothioate diester and a single deoxynucleotide (13dC69s, 5′–CUUAGdCsUCCACCA-3′) was used for the covalent attachment of a photoaffinity probe. A modification of the procedure described by Fidanza and McLaughlin (1989) for the incorporation of reporter groups into DNA oligonucleotides was employed (Fidanza & McLaughlin, 1989). A single deoxynucleotide was incorporated at the position immediately 5′ to the phosphorothioate triester to avoid probe elimination by the ribose 2′-hydroxyl (Gish & Eckstein, 1988). Immediately before use, a 30 mM stock solution of 4-(iodoacetamido)-benzophenone (BPIA) (Molecular Probes, Eugene, OR) was prepared in ethanol. The concentration was estimated using an ϵ_{300} of 23 000 M^{-1} cm^{-1} (Molecular Probes). Labeling reactions and other manipulations prior to photolysis were carried out in the dark or under dim lighting. Labeling was performed in 60% ethanol using a 58-fold excess probe (16.2 mM final BPIA) over oligonucleotide (278 μM final 13dC69s) in a reaction volume of 1 mL at pH 6–7. Reactions were carried out at 50 °C for 24 h, and labeling yields were estimated to be 40–60%. Purification of the labeled product oligonucleotide was achieved by HPLC either on a C18 reverse-phase column (Vydac) equilibrated in 0.1 M triethylammonium acetate (pH 7.0) and eluted with an acetonitrile (0–50% over 50 min) gradient or on a Progel-TSK DEAE-2SW column (Supelco, Inc.) equilibrated in 20 mM sodium acetate and 20% acetonitrile (pH 6.5) and eluted with a linear gradient of 0–1.5 M KCl over 50 min (Webster et al., 1991). The absorbance at 260 nm was used to monitor the elution profile. Both methods resulted in the separation of unlabeled tridecamer from BP-labeled tridecamer, but recovery of RNA was typically higher using the latter approach. Peaks were collected separately and dried down in a speed vac. Products eluted from the DEAE column were desalted on a Sep-Pak C18 cartridge (Millipore). Final overall yields of BP-labeled tridecamer after HPLC and Sep-Pak purification were 25–30%.

A comparison of the relative mass of the HPLC-purified BP-labeled oligomer with that of the unlabeled oligomer was made using laser desorption mass spectrometry. The expected mass difference of 240, corresponding to a single covalently bound benzophenone moiety, was obtained. Mass spectral data were provided by the MIT Mass Spectrometry Facility.

[1] Abbrevations: AlaRS, alanyl-tRNA synthetase; BP, benzophenone; BPIA, 4-(iodoacetamido)benzophenone; kDa, kilodaltons; 13dC69s, tridecamer oligoribonucleotide (5′-CUUAGdCsUCCACCA-3′) containing a single deoxycytidine and a single phosphorothioate.

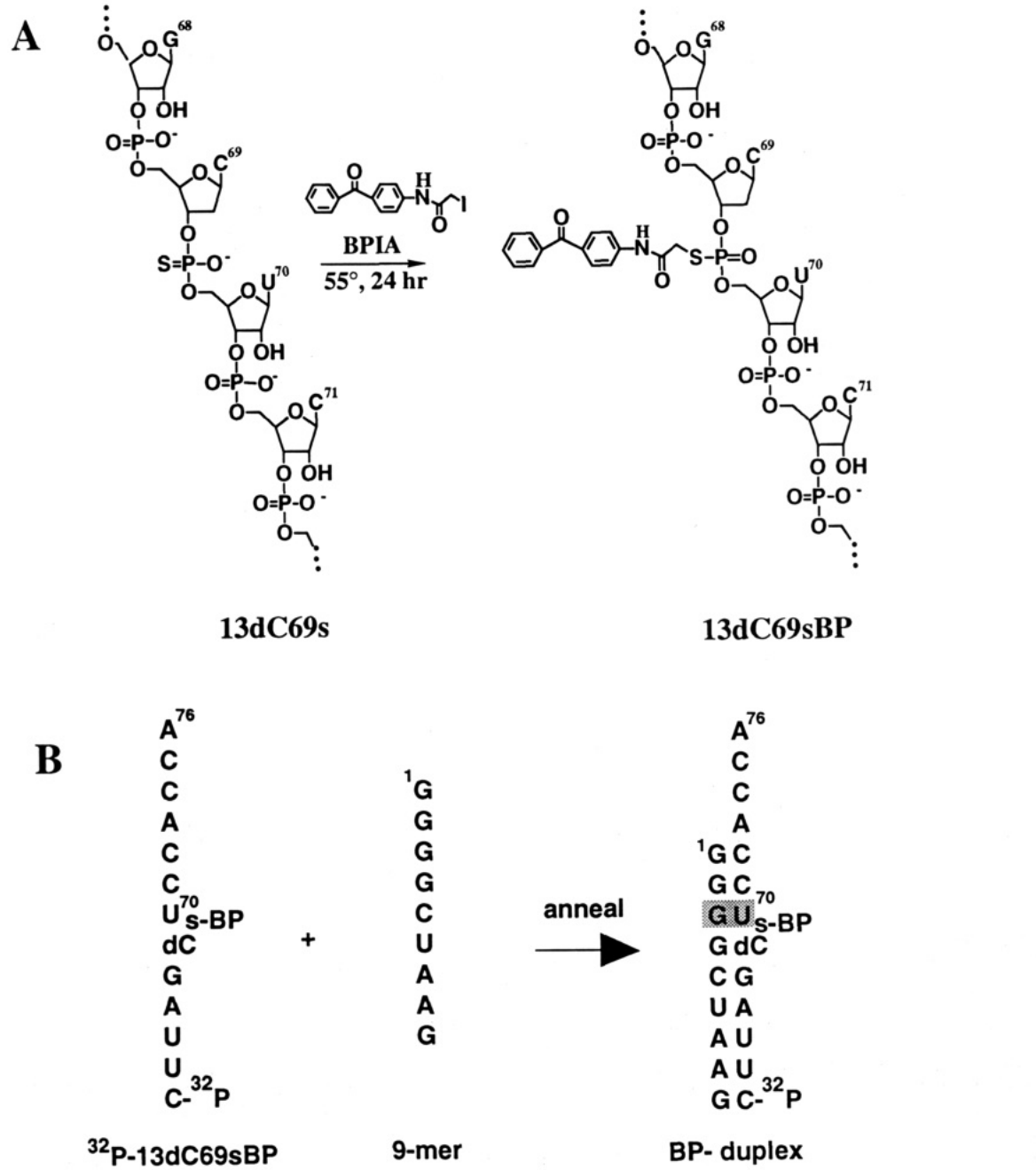

FIGURE 1: Introduction of a benzophenone (BP) photoaffinity probe into a synthetic mixed oligonucleotide. A shows the partial structure of the tridecamer (13dC69s) and the site of probe attachment. B shows the preparation of the BP-labeled duplex substrate. The sequence is based on the acceptor stem of full-length $tRNA^{Ala}$.

Photoaffinity Cross-Linking. The benzophenone-labeled tridecamer (13dC69sBP) was 5′-^{32}P-end-labeled and gel-purified using standard protocols (Maniatis et al., 1982). Cross-linking experiments were performed as follows. Duplexes were first obtained by combining 100 μM [^{32}P]13dC69sBP with an equimolar amount of complementary 5′-strand ribononamer in 50 mM sodium phosphate at pH 7.0–7.5. The oligonucleotides were annealed by heating to 80–90 °C for 3 min and cooling on ice. The annealed duplex (25 μM) was then combined with alanyl-tRNA synthetase (2 μM) in a reaction buffer containing 50 μM sodium phosphate (pH 7.0–7.5) and 5–10 mM $MgCl_2$. Analytical-scale cross-linking was performed in 20–80-μL reaction volumes, while preparative-scale reaction volumes were 1–4 mL. Photolysis was carried out in silanized pyrex tubes that were suspended in the middle of a Rayonet RMR-500 photochemical minireactor (The Southern New England Ultraviolet Company). The light source consisted of four RPR 3500-Å lamps (4.5 W), and photolysis was performed at 4 °C for 2 h. To visualize and quantitate the extent of cross-linking, radioactive standards were electrophoresed on SDS–polyacrylamide gels along with an aliquot of the cross-linked sample. The amount of radioactivity incorporated into the band corresponding to AlaRS was quantitated using a phosphorimager.

Inactivation and Protection Studies. The aminoacylation activity of AlaRS was monitored as a function of the time of photolysis in the absence and presence of BP-labeled duplex. Photolysis was performed as above in 50 mM sodium phosphate, (pH 7.5), 10 mM $MgCl_2$, and 0.1 mg/mL BSA with 0.1 μM AlaRS and 20 μM BP-labeled duplex. In order to assess the cross-linking specificity, some reactions were preincubated with either 100 μM cognate substrate (G3:U70 minihelix Ala) or noncognate substrates (G3:C70 minihelix Ala, random RNA 16-mer) before the addition of BP-labeled duplex and subsequent photolysis. Aliquots were removed at

various times during photolysis, and the enzyme was assayed for its ability to aminoacylate $tRNA^{Ala}$.

Peptide Isolation and Sequencing. Following photolysis, samples were eluted through Centricon 30 concentrators (Amicon) to remove the bulk of free RNA. Partial tryptic digests were performed in 50 mM sodium phosphate (pH 7.5) and 0.15 mM $CaCl_2$. RNase-free trypsin was added at an enzyme:substrate ratio of 1:25 (w:w), and the mixture was incubated for 3 h at 37 °C. Visualization and quantitation of cross-linked tryptic fragments were achieved by analysis on 15% SDS–polyacrylamide gels and phosphorimaging as described above. For sequence analysis, peptides were electroblotted from polyacrylamide gels onto a poly(vinylidine difluoride) membrane (Millipore) and sequenced directly as described (Matsudaira, 1987). Total tryptic digests were performed as above, except for the addition of 3 M urea to the digestion buffer and a longer incubation time of 12–16 h at 37 °C.

RESULTS

Probe Preparation. As shown in Figure 1, a single benzophenone photoaffinity reporter group has been covalently attached to a chemically synthesized mixed oligonucleotide tridecamer containing a single phosphorothioate diester and a single deoxynucleotide. The sequence of this primarily RNA tridecamer corresponds to the 3′-end of $tRNA^{Ala}$. The coupling of BPIA to the oligomer proceeded with yields of up to 60% after 24 h at 50 °C. Similar results have been previously obtained for the attachment of reporter groups to all-DNA oligonucleotides (Fidanza & McLaughlin, 1989; Fidanza et al., 1992). Incorporation of a single deoxynucleotide at position C69 of the primarily ribonucleotide oligomer was found to be essential for the stability of the covalent modification.

The probe elimination that resulted when BP labeling was attempted with an all-RNA oligomer was most likely the result of nucleophilic addition of the 2′-hydroxyl of the cytidine to the labeled phosphorus atom (Gish & Eckstein, 1988). The absorbance spectrum of the HPLC-purified BP-labeled oligomer shows an absorbance shoulder at 300 nm corresponding to the BP moiety. An approximate labeling stoichiometry of 1:1 was calculated using an ϵ_{300} of 23 000 $M^{-1}\,cm^{-1}$. Mass spectral analysis confirmed a ratio of one BP per RNA molecule.

Annealing to a complementary 5′-ribononamer results in an active alanine-accepting substrate for AlaRS (Figure 1B). As previously shown, the presence of a single deoxynucleotide at position C69 has no effect on the aminoacylation of duplex substrates (Musier-Forsyth & Schimmel, 1992). Furthermore, the attachment of the benzophenone label on the RNA backbone in the position between bases dC69 and U70 results in only a 2.7-fold reduction in the initial rate of aminoacylation (Figure 2).

Photo-Cross-Linking. Upon photolysis at long wavelengths (>320 nm), aromatic ketones such as benzophenone convert to the triplet state that is inert toward water, but has the capability of reacting with either proteins or nucleic acids through hydrogen atom abstraction–addition reactions (Galardy & Craig, 1972). Activation is easily achieved with low-intensity lamps, and high cross-linking yields have been obtained with little, if any, protein destruction (Parker & Hodges, 1984, 1985; Williams et al., 1986). The effectiveness of the 350-nm light source used in these experiments for activating the BP-labeled RNA was first assessed by monitoring the decrease in the absorbance of the probe at 300 nm as a function of the time of photolysis at 4 °C. Maximum

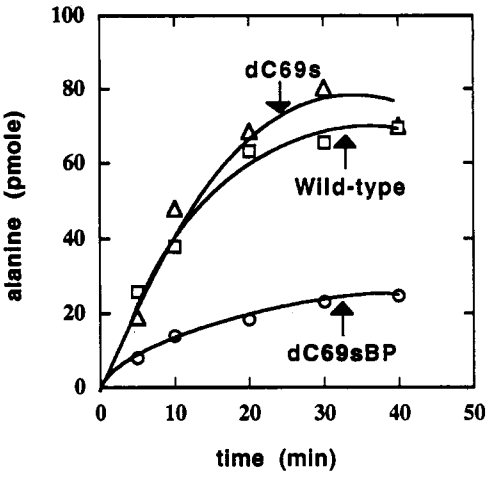

FIGURE 2: Aminoacylation with the alanine of miniduplex substrates by AlaRS at pH 7.5 and 25 °C. The assay compares the relative activity of the unmodified duplex (wild-type) to the singly deoxy- and phosphorothioate-substituted duplex (dC69s) and to the fully modified BP-labeled duplex (dC69sBP).

reduction in A_{300} was achieved in about 2 h, and this was the irradiation time used in all cross-linking experiments.

Photolysis of AlaRS in the presence of BP-labeled duplex resulted in the incorporation of radioactivity into AlaRS as visualized by SDS–polyacrylamide gel electrophoresis and autoradiography. A radioactive band that eluted at approximately the same position as AlaRS on a Coomassie Blue stained gel (about 96 kDa) was observed (Figure 3, lane 2). This band was identified as cross-linked AlaRS–RNA by performing the following control experiments. The appearance of the band was light-dependent (Figure 3, lanes 1 and 2) and AlaRS-dependent. Furthermore, the band did not appear upon photolysis of AlaRS with [^{32}P]duplex in the absence of photoprobe. Cross-linking yields were typically 10–12%, as determined by measuring the incorporation of radioactivity into the AlaRS band by phosphorimaging. Coomassie staining or autoradiography did not show any significant amount of protein material in the wells (indicative of aggregation).

To assess the functional importance and specificity of the site(s) of cross-linking, the aminoacylation activity of AlaRS was monitored during a period of photolysis in the presence and absence of the photoprobe (data not shown). Photolysis of 2 μM AlaRS for 60 min in the absence of photoprobe resulted in only a 2% loss of enzymatic activity. Photolysis in the presence of 25 μM BP-labeled duplex, however, resulted in up to 52% inactivation. The fact that this loss exceeds the amount of cross-linking, as determined by the incorporation of radioactivity into AlaRS, may be explained by degradation of the ^{32}P-end-labeled RNA probe during the course of the experiment. The specificity of cross-linking was examined further by measuring enzymatic activity as a function of photolysis in the presence of BP-labeled duplex and cognate or noncognate substrates (data not shown). The G3:U70 minihelix is able to protect the enzyme completely from BP-dependent inactivation, while the G3:C70 minihelix and a random RNA 16-mer afforded no protection (data not shown).

Peptide Isolation and Identification. Studies were carried out to determine which regions of the protein are cross-linked to the RNA. Proteolytic fragments of the cross-linked complex were generated with trypsin and analyzed by electrophoresis on SDS–polyacrylamide gels. Five radioactive fragments were seen after a partial tryptic digest (Figure 3, lane 3). The distribution of radioactivity in these fragments was quantitated by phosphorimaging. Approximately 50% of the radioactivity is incorporated into an 18-kDa fragment, 20% into a 48-kDa

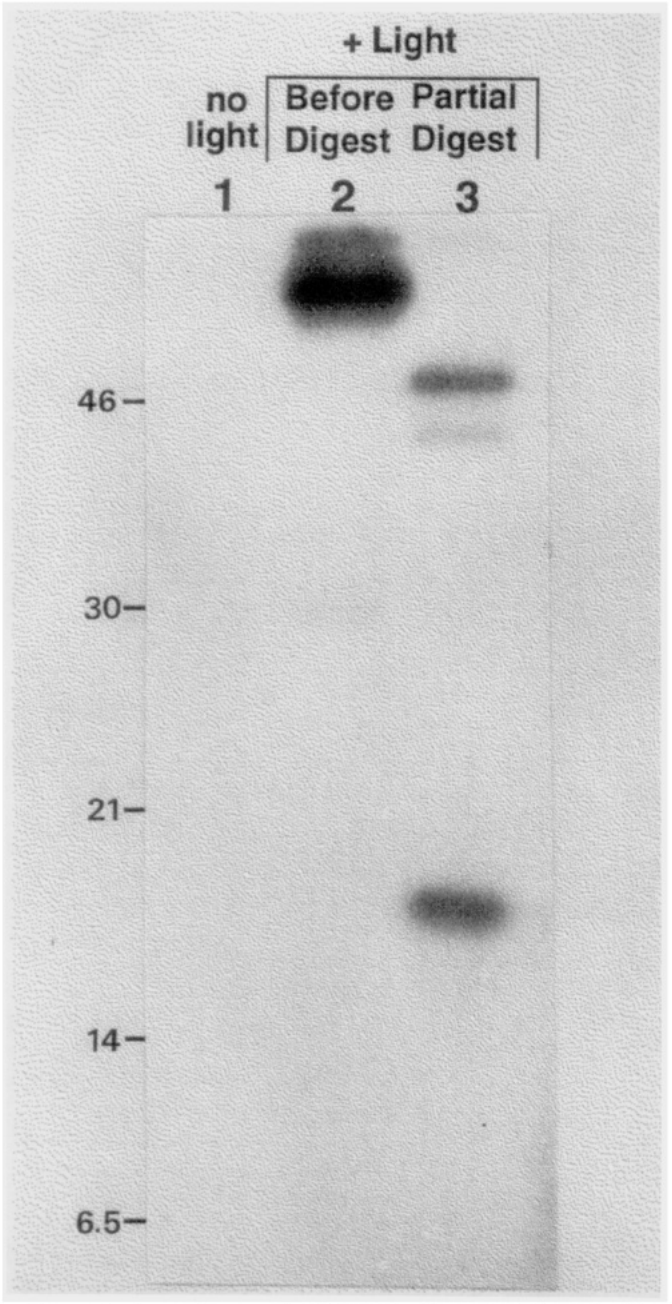

FIGURE 3: Autoradiogram of a 15% SDS–polyacrylamide gel showing the results of a photoaffinity cross-linking experiment: lane 1, AlaRS and BP-labeled duplex incubated in the dark for 2 h; lane 2, AlaRS and BP-labeled duplex after 2 h of photolysis; lane 3, partial tryptic digest of the photolyzed complex.

fragment, and 10% into each of three minor fragments of about 44, 16, and 12 kDa. The latter two bands are not clear in the partial digest shown in Figure 3, probably due to partial degradation of the radioactive end label in this particular experiment. Only a single band that coeluted with the 44-kDa radioactive fragment was observed by either Coomassie Blue or silver staining of polyacrylamide gels following partial proteolysis. As previously shown, this 44-kDa fragment corresponds to a stable N-terminal tryptic fragment of 368 amino acids, which is sufficient for aminoacyl adenylate synthesis, but not for aminoacylation (Herlihy et al., 1980; Regan et al., 1987; Hsieh & Campbell, 1991). (We estimate that the BP-labeled 13-mer contributes approximately 4.5 kDa to the molecular weight of the fragment–RNA complexes resolved by the SDS gel electrophoresis.) Under conditions of partial proteolysis, the 368-mer is normally extremely resistant to further degradation by trypsin. The 18-kDa

Table 1: Amino-Terminal Sequence of the Miniduplex-Labeled Peptides

cycle	major residue	pmol detected[a] 12 kDa	16 kDa	18 kDa	AlaRS sequence
1	X[b]				G161
2	A	159.7	20.3	15.4	A*[c]
3	P	93.7	13.7	9.8	P*
4	Y	121.0	12.3	8.6	Y*
5	A	108.0	11.2	8.7	A*
6	S	27.7	4.0	2.7	S*
7	D	56.7	5.1	6.1	D*
8	N	40.0	3.8	3.8	N*
9	F	42.2	3.9	3.7	F*
10	A	2.3	ND[d]	0.6	W
11	Q	27.6	2.6	1.9	Q*
12	M	32.2	1.3	1.1	M*

[a] Peptide–duplex complexes corresponding to the molecular weight indicated were electroblotted from polyacrylamide gels and sequenced directly. The contribution to the molecular weight of the cross-linked 13-nucleotide, benzophenone-labeled RNA single strand is approximately 4.5 kDa. [b] X indicates that the background was too high to determine the residue at this cycle. [c] Asterisks indicate that the peptide seqeunce matches the AlaRS sequence. [d] ND, not detected.

fragment obtained as the major fragment of partially proteolyzed cross-linked AlaRS is derived from an internal portion of the 368-mer (see below). Trypsin can apparently gain access to sites necessary for generating this fragment more readily in cross-linked species of the full-length protein.

Following digestion, approximately 70% of the label was attached to the three shorter proteolytic fragments of 12, 16, and 18 kDa. These bands were blotted onto PVDF membranes and submitted for N-terminal sequence analysis. Each of the fragments contained a major peptide, and in two of the fragments additional minor peptide sequences were also obtained (Table 1). In each case, the 12 N-terminal amino acids of the major peptide are XAPYASDNFXQM, which matches residues 161–172 of AlaRS (Table 1 and Figure 4). While glycine was present in cycle 1, an amino acid assignment could not be made definitively due to the high background signal in this cycle. Furthermore, difficulties in the correct identification of tryptophan (cycle 10) are not uncommon in sequence analyses. Due to the presence of the RNA label, which may affect the mobility of the peptides on SDS gels, the exact length of the sequenced fragments is difficult to estimate. However, on the basis of protein molecular weight standards and the 4.5-kDa contribution of the BP-labeled RNA 13-mer, the smallest of these fragments is estimated to be on the order of 60–70 amino acids. Within the 12 cycles of the major peptide that were sequenced, the analyses did not identify a radioactive cycle or an anomalous peak corresponding to the signal, which might be obtained from a covalently modified residue. This is not an unexpected result due to the length of the fragments and the relatively harsh conditions employed for the blotting and sequencing reactions, which are likely to result in the destruction of the ^{32}P-end-labeled RNA probe.

A cross-linking experiment was also carried out with an active truncated version of AlaRS containing only the 461 N-terminal amino acids. A yield of cross-linking was obtained that was very similar to the full-length enzyme. This experiment confirms that the major site of interaction with the RNA probe is with the N-terminal portion of AlaRS.

In an attempt to isolate shorter cross-linked peptides, total tryptic digests were prepared and analyzed on 15–20% SDS–polyacrylamide gels. A single radioactive band, which migrated as a 4-kDa species, was seen. However, a clean peptide sequence was not obtained from a PVDF blot of this fragment due to the presence of a number of contaminating

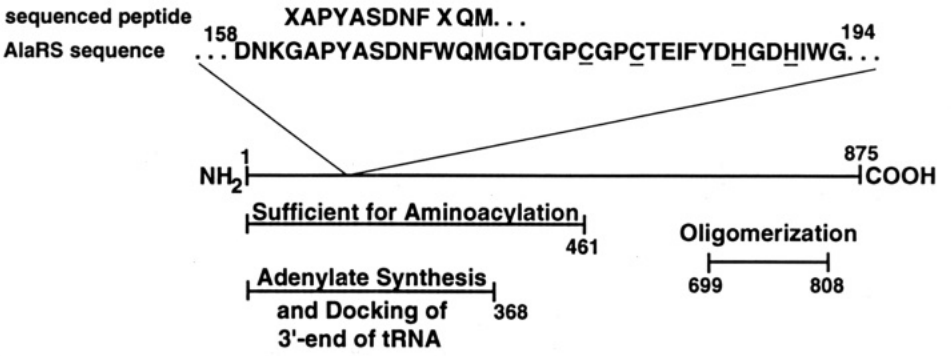

FIGURE 4: Schematic representation of AlaRS showing the sequence and relative location of the sequenced peptide cross-linked to the BP-labeled duplex. The functional domains of AlaRS are also indicated.

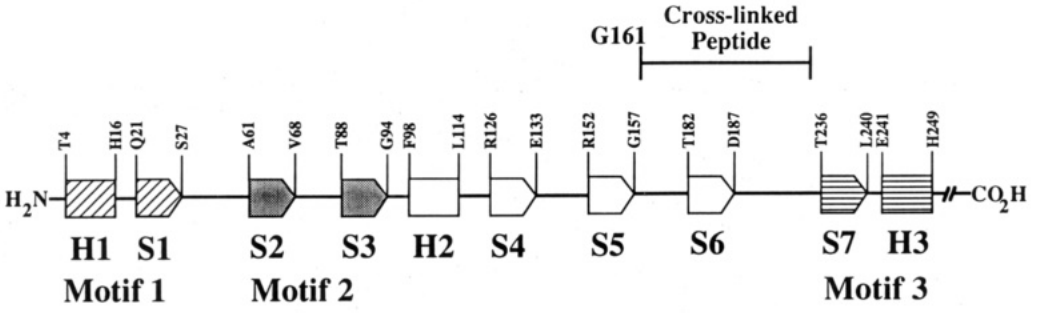

FIGURE 5: Linear depiction of the active-site secondary structure of AlaRS showing the location of the cross-linked peptide [see Ribas de Pouplana (1993)]. Rectangles and cylinders denote α-helices and arrows denote β-strands. The residue numbers at the beginning and end of each strand and helix are indicated. The class-defining sequence motifs are shaded and labeled.

peptides that coeluted at this position in the gel. Several attempts were made to purify cross-linked peptides by HPLC using both reverse-phase and anion-exchange chromatography. However, large losses in the ^{32}P signal were observed at each step. This is probably due to degradation of the ^{32}P-end-labeled RNA probe combined with losses due to the retention of RNA on the columns.

DISCUSSION

The attachment of the benzophenone label at the C69–U70 internucleotide linkage (Figure 1) results in a substrate with activity comparable to that of the unmodified RNA (Figure 2). This circumstance was favorable for the formation of an active enzyme–RNA complex, but also suffers from the disadvantage that, in this location, the probe must not be on exactly the same side of the helix as the bound enzyme. In addition, it should also be noted that two phosphorus diastereomers (S_P and R_P) result from chemical modification of the prochiral phosphodiester residue. Two orientations of the BP group were, therefore, employed throughout these cross-linking experiments. In addition, the length of the cross-linker is estimated as 12–14 Å. This method was, therefore, not designed to identify a critical contact directly, but was useful in locating a region of AlaRS that may contain functionally important amino acid side chains.

Although the three-dimensional structure of AlaRS is unknown, the secondary structure has been modeled for the portion of the active-site domain that encompasses the three sequence motifs characteristic of class II enzymes (Ribas de Pouplana et al., 1993). The modeling was based in part on the alignment of six sequences for alanine tRNA synthetases in conjunction with the neural network-based prediction program PHD of Rost and Sander (1992) and on the shared conserved structural motifs in the related class II aspartyl- and seryl-tRNA synthetases (Cusack et al., 1990; Ruff et al., 1991). This conserved structure consists of seven β-strands (S1–S7) with three α-helices (H1–H3). In this model of the secondary structure, the peptide cross-linked to the benzophenone affinity label at the G3:U70 base pair starts at the beginning of the segment between S5 and S6 and extends into the piece between S6 and S7 (Figure 5). This peptide segment includes a putative zinc-binding site, which starts at Cys178 and has been implicated in acceptor helix recognition (Miller & Schimmel, 1992).

In the cocrystal of aspartate tRNA synthetase with $tRNA^{Asp}$, acceptor helix contacts are made by amino acids in the loop between S4 and S5 and the loop between the two β-strands of motif 2 (Cavarelli et al., 1993). While neither of these regions is part of the cross-linked peptide in the AlaRS system, and while this result may reflect the inherently imprecise nature of the probe referred to above and errors in the secondary structure prediction, the conserved structural elements between motifs 2 and 3 are joined together by polypeptide segments of variable sizes (Eriani et al., 1990). We propose that, in addition to or as an alternative to the loop between strands S4 and S5, the loops joining S5 to S6 and S6 to S7 may, in some synthetases, provide acceptor helix contacts.

Motifs 2 and 3 provide contacts with ATP and presumably also contact the aminoacyl adenylate (Cusack et al., 1990; Moras, 1992). The loop between the two β-strands of motif 2 in aspartate tRNA synthetase interacts with the discriminator base G73 and the first base pair of the acceptor stem of $tRNA^{Asp}$ (Cavarelli et al., 1993). These interactions of the loop of motif 2 with the acceptor end of the tRNA substrate are not surprising for a peptide that is proximal to the activated amino acid. Lys73 is located within the analogous segment between the β-strands of motif 2 of AlaRS (Figure 5), and this lysine was cross-linked to the 3′-end of periodate-oxidized $tRNA^{Ala}$ (Hill & Schimmel, 1989). While the loop between the β-strands of motif 2 interacts with the end of the bound tRNA, possibly one or more of the segments between S5, S6, and S7 have contacts further within the acceptor stem.

The crystal structures of a class I and a class II synthetase–tRNA complex (Rould et al., 1989; Ruff et al., 1991), and

the results reported here, each show that sequences within the catalytic domain of aminoacyl tRNA synthetases have been incorporated to accommodate tRNA acceptor stems. These sequences appear to be idiosyncratic to the synthetase and are not a part of the actual conserved structure within which they are embedded. Genetic studies of Meinnel et al. of *E. coli* methionine tRNA synthetase (Meinnel et al., 1991) are also consistent with the interpretation that acceptor helix interactions arise from contacts directly or indirectly due to an insertion [designated as CP1 (Starzyk et al., 1987)] into the nucleotide binding fold, which typifies the class I active-site domain (Schimmel, 1991). Possibly, the primordial synthetase of each class consisted of the conserved active-site domain which catalyzed amino acid activation. Insertions into this domain allowed interactions with RNA structures that were the progenitors of transfer RNAs (Schimmel et al., 1993). These interactions may have been constrained to just nucleotides close to the 3′-end of the RNA because of the small size of the early synthetase and formed the basis of an operational RNA code for amino acids. This code is reflected in contemporary synthetases by their sequence-specific aminoacylation of RNA oligonucleotides.

ACKNOWLEDGMENT

We thank Dr. Douglas Buechter for preparation of the truncated (461-mer) form of AlaRS used in this study and for many helpful discussions. Protein sequence analyses were performed by Chuck Burkins at the Whitehead Protein Sequencing Facility (Cambridge, MA) and by Richard F. Cook at the MIT Biopolymers Lab. Mass spectral data were provided by the MIT Mass Spectrometry Facility, which is supported by NIH Grant No. RR00317 (to K. Biemann).

REFERENCES

Brunie, S., Zelwer, C., & Risler, J.-L. (1990) *J. Mol. Biol. 216,* 411–424.
Buechter, D. D., & Schimmel, P. (1993) *Biochemistry 32,* 5267–5272.
Cavarelli, J., Rees, B., Ruff, M., Thierry, J.-C., & Moras, D. (1993) *Nature 362,* 181–184.
Cusack, S., Berthet-Colominas, C., Härtlein, M., Nassar, N., & Leberman, R. (1990) *Nature 347,* 249–265.
Eriani, G., Delarue, M., Poch, O., Gangloff, J., & Moras, D. (1990) *Nature 347,* 203–206.
Fersht, A. R., Ashford, J. S., Bruton, C. J., Jakes, R., Koch, G. L. E., & Hartley, B. S. (1975) *Biochemistry 14,* 1–4.
Fidanza, J. A., & McLaughlin, L. W. (1989) *J. Am. Chem. Soc. 111,* 9117–9119.
Fidanza, J. A., Ozaki, H., & McLaughlin, L. W. (1992) *J. Am. Chem. Soc. 114,* 5509–5517.
Francklyn, C., & Schimmel, P. (1989) *Nature 337,* 478–481.
Francklyn, C., & Schimmel, P. (1990) *Proc. Natl. Acad. Sci. U.S.A. 87,* 8655–8659.
Francklyn, C., Shi, J.-P., & Schimmel, P. (1992) *Science 255,* 1121–1125.
Frugier, M., Florentz, C., & Giegé, R. (1992) *Proc. Natl. Acad. Sci. U.S.A. 89,* 3990–3994.
Galardy, R. E., & Craig, L. C. (1972) *Nature New Biol. 242,* 127–128.
Gish, G., & Eckstein, F. (1988) *Science 240,* 1520–1522.
Herlihy, W., Royal, N. J., Biemann, K., Putney, S., D., & Schimmel, P. R. (1980) *Proc. Natl. Acad. Sci. U.S.A. 77,* 6531–6535.
Hill, K., & Schimmel, P. (1989) *Biochemistry 28,* 2577–2586.
Hou, Y.-M., & Schimmel, P. (1988) *Nature 333,* 140–145.
Hou, Y.-M., & Schimmel, P. (1989) *Biochemistry 28,* 6800–6804.
Hsieh, H. L., & Campbell, D. R. (1991) *Biochem. J. 278,* 809–816.
Maniatis, T., Fritsch, E. F., & Sambrook, J. (1982) *Molecular Cloning: A Laboratory Manual,* Cold Spring Harbor Laboratory Press, Cold Spring Harbor , NY.
Martinis, S. A., & Schimmel, P. (1992) *Proc. Natl. Acad. Sci. U.S.A. 89,* 65–69.
Matsudaira, P. (1987) *J. Biol. Chem. 262,* 10035–10038.
McClain, W. H., & Foss, K. (1988) *Science 240,* 793–796.
Meinnel, T., Mechulam, Y., Le Corre, D., Panvert, M., Blanquet, S., & Fayat, G. (1991) *Proc. Natl. Acad. Sci. U.S.A. 88,* 291–295.
Miller, W. T., & Schimmel, P. (1992) *Proc. Natl. Acad. Sci. U.S.A.* 89, 2032–2035.
Miller, W. T., Hou, Y.-M., & Schimmel, P. (1991) *Biochemistry 30,* 2635–2641.
Milligan, J. R., Groebe, D. R., Witherell, G. W., & Uhlenbeck, O. C. (1987) *Nucleic Acids Res. 15,* 8783–8798.
Moras, D. (1992) *Trends Biochem. Sci. 17,* 159–164.
Musier-Forsyth, K., & Schimmel, P. (1992) *Nature 357,* 513–515.
Musier-Forsyth, K., Scaringe, S., Usman, N., & Schimmel, P. (1991a) *Proc. Natl. Acad. Sci. U.S.A. 88,* 209–213.
Musier-Forsyth, K., Usman, N., Scaringe, S., Doudna, J., Green, R., & Schimmel, P. (1991b) *Science 253,* 784–786.
Nureki, O., Niimi, T., Muto, Y., Kanno, H., Kohno, T., Muramatsu, T., Kawai, G., Miyazawa, T., Giege, R., Florentz, C., & Yokoyama, S. (1993) *The Translation Apparatus* (Nierhaus, K., Ed.) Springer-Verlag, Berlin (in press).
Parker, J. M. R., & Hodges, R. S. (1984) *J. of Protein Chem. 3,* 465–478.
Parker, J. M. R., & Hodges, R. S. (1985) *J. of Protein Chem. 3,* 479–489.
Regan, L., Bowie, J., & Schimmel, P. (1987) *Science 235,* 1651–1653.
Ribas de Pouplana, L., Buechter, D. D., Davis, M. W., & Schimmel, P. (1993) *Protein Sci.* (in press).
Rich, A., & RajBhandary, U. L. (1976) *Annu. Rev. Biochem. 45,* 805–860.
Rost, B., & Sander, C. (1992) *Nature 360,* 540.
Rould, M. A., Perona, J. J., Söll, D., & Steitz, T. A. (1989) *Science 246,* 1135-1142.
Rould, M. A., Perona, J. J., Söll, D., & Steitz, T. A. (1991) *Nature 352,* 213–218.
Ruff, M., Krishnaswamy, S., Boeglin, M., Poterszman, A., Mitschler, A., Podjarny, A., Rees, B., Thierry, J. C., & Moras, D. (1991) *Science 252,* 1682–1689.
Sampson, J. R., & Saks, M. E. (1993) *Nucleic Acids Res. 21,* 4467–4475.
Scaringe, S. A., Francklyn, C., & Usman, N. (1990) *Nucleic Acids Res. 18,* 5433–5441.
Schimmel, P. (1987) *Annu. Rev. Biochem. 56,* 125–158.
Schimmel, P. (1991) *Curr. Opin. Struct. Biol. 1,* 811–816.
Schimmel, P., Giege, R., Moras, D., & Yokoyama, S. (1993) *Proc. Natl. Acad. Sci. U.S.A.* (in press).
Shi, J.-P., Francklyn, C., Hill, K., & Schimmel, P. (1990) *Biochemistry 29,* 3621–3626.
Shi, J.-P., Martinis, S. A., & Schimmel, P. (1992) *Biochemistry 31,* 4931–4936.
Starzyk, R. M., Webster, T. A., & Schimmel, P. (1987) *Science 237,* 1614–1618.
Trezeguet, V., Edwards, H., & Schimmel, P. (1991) *Mol. Cell. Biol. 11,* 2744–2751.
Webster, K. R., Shamou, Y., Konigsberg, W., & Spiar, E. K. (1991) *Biotechniques 11,* 658–661.
Williams, N., Ackerman, S. H., & Coleman, P. S. (1986) *Methods Enzymol. 126,* 667–682.